Journal of the Serbian Chemical Society
JSCS-info@shd.org.rs • www.shd.org.rs/JSCS
J. Serb. Chem. Soc. *88* (7–8) 685–704 (2023)
JSCS–5655
Survey
Published 6 August, 2023

SURVEY

Application aspects of joint anaphoresis/substrate anodization in production of biocompatible ceramic coatings

KATARINA Đ. BOŽIĆ[1,2#], MIROSLAV M. PAVLOVIĆ[1,2*#], GAVRILO M. ŠEKULARAC[1], STEFAN V. PANIĆ[1] and MARIJANA R. PANTOVIĆ PAVLOVIĆ[1,2#]

[1]*Institute of Chemistry, Technology and Metallurgy, National Institute of the Republic of Serbia, Department of Electrochemistry, University of Belgrade, Belgrade, Serbia and* [2]*Center of Excellence in Environmental Chemistry and Engineering, Institute of Chemistry, Technology and Metallurgy, Belgrade, Serbia*

(Received 18 January, revised 10 February, accepted 8 July 2023)

Abstract: Electrophoretic deposition (EPD) occurs as a cataphoretic deposition – the coating is deposited on the cathode, and anaphoretic deposition – the coating is deposited on the anode. The primary purpose of EPD is to obtain compact and uniform organic/inorganic coatings of the desired thickness and adhesion on metal surfaces by applying an electric field to the particles of coating precursor. EPD basic principles for coatings deposition concerning fundamental explanations and considerations of practical parameters of the process are presented. Cataphoretic deposition has become popular because it can apply organic coatings to complex structures that are otherwise very difficult to coat. These coatings were found to improve the characteristics of the substrate, such as biocompatibility, appearance and resistance to the corrosion processes. The key EPD parameters are composition, pH value and viscosity of deposition medium, as well as zeta potential of the particles, electric field strength, *etc*. A special survey is given to the process of anaphoretic deposition, which is relatively new, and its advantages over cataphoretic deposition are discussed. Through the process of joint anaphoresis/substrate anodization process, the surface of the substrate is simultaneously anodized and modified by incorporation of the foreign particles into the anodic layer. The coatings of mixed composition of better adhesion and corrosion resistance with respect to cataphoretically-deposited coatings are obtained as result.

Keywords: biomedical implants; titanium; anodization; cataphoresis; anaphoresis.

* Corresponding author. E-mail: miroslav.pavlovic@ihtm.bg.ac.rs
# Serbian Chemical Society member.
https://doi.org/10.2298/JSC230118034B

CONTENTS

1. INTRODUCTION

Various techniques are used to apply inorganic/organic composite coatings to metal substrates: the sol–gel process,[1] dip coating,[2] aerosol deposition/plasma spraying[3,4] and layer-by-layer deposition.[5] Electrophoretic deposition (EPD) has attracted attention as a simple and economical process which offers the possibility of applying uniform coatings on substrates of complex shapes at room temperature.[6] In EPD, the charged particles in suspension are attracted to and deposited on an oppositely charged electrode (substrate).[7]

EPD is a flexible technique suitable for the application of polymers, ceramics and composites. EPD involves two processes, electrophoresis and deposition. A positive or negative charge spontaneously generated on the surface of suspended particles, induces the particle movement towards the oppositely charged electrode as a pole of the applied electric field, in a process known as electrophoresis. Some materials already have a charge on their surface due to the presence of specific functional groups, or a species charge can be generated by adding to the suspension the ions of high adsorption ability. The second process is the coagulation of charged particles while they are depositing on the surface of the oppositely charged electrode. Consequently, a relatively compact and homogeneous coating is formed. The most straightforward apparatus for performing the EPD process consists of two parallel electrodes connected to a power source and immersed in a suspension of depositing particles.[8]

The EPD process can be cathodic (cataphoretic deposition) or anodic (anaphoretic deposition), depending on the electrode on which the deposition occurs,

according to the sign of the charge at particle surface. When the particles are positively charged, the deposition occurs on the cathode (negative electrode), and the process is called cathodic EPD. Anodic EPD is defined as the deposition of negatively charged particles on the anode (positive electrode).[7] Two types of electric fields can be applied for this process, alternating (AC) or direct (DC).[8]

2. FACTORS AFFECTING EPD

Two groups of parameters influence the EPD process: suspension-related parameters and process-related parameters. One of the most critical parameters for the deposition of uniform coatings is the formation of a stable suspension with well-dispersed charged particles. Particles are suspended in a medium by the interplay of three different forces: van der Waals attractive force, electrostatic repulsive force and a steric force of coagulate formation (not always present). For a suspension to be stable, electrostatic repulsive and/or steric forces must be dominant over van der Waals attraction. The charged particles move towards the appropriate electrode, where they are then electrostatically deposited upon charge neutralization.[7]

The main electrophoretic characteristic of a particle under the influence of an electric field is electrophoretic mobility.[9] Factors that affect the mobility of charged particles are mostly related to the particle characteristics in the specific suspending medium. Electrophoretic mobility (μ) is defined by Henry equation:[10]

$$\mu = \frac{2}{3}\frac{\varepsilon_0 \varepsilon_r \zeta}{\eta} f(\kappa r) \quad (1)$$

where ε_0 is the electric permittivity of vacuum, ε_r is the relative electric permittivity of the suspending medium, ζ is the zeta potential, η is the solvent viscosity, $f(\kappa r)$ is the Henry coefficient, which depends on the relation between the thickness of the double layer ($1/\kappa$) which is created between the electrode surface and charged particles, and the core radius (r) of the particle.

According to Eq. (1), the electrophoretic mobility of a particle is directly proportional to the electric permittivity of the suspending medium, the potential gradient, *i.e.*, the zeta potential at the particle surface, and it is inversely proportional to the viscosity of the suspension.

2.1. Key parameters related to the suspension

2.1.1. Particle size

The size of the particles deposited by the EPD method is an important parameter. The finely suspended particles are crucial for obtaining a uniform coating. Particle size and morphology directly affect the particle electrophoretic mobility, the coating thickness and the zeta potential.[11] It has been found that for many ceramic systems, a particle size of 1–20 μm leads to good deposit properties.[9] The increase in the size of the particles leads to suspension inhomo-

geneity and their precipitation due to the influence of gravity, causing an uneven coating thickness. In these cases, the mobility of the particles due to electrophoresis must be greater than the mobility of the particles under the influence of the gravitational field. Small particles have a large electrophoretic mobility. However, if there are larger particles in the suspension, it is necessary to apply a strong electric field or to increase the zeta potential to achieve good electrophoretic mobility.[8] The reduction in particle size also allows better control of cracks that may occur due to coating shrinkage during the drying phase.[12]

2.1.2. Dielectric constant of the liquid

The dielectric constant of the suspending medium should have an optimum value. Liquids with a low dielectric constant value cause low mobility, and therefore no deposition can occur. At high values of the dielectric constant, the thickness of the electric double layer decreases due to the high concentration of polar solvent molecules within, which also reduces the electrophoretic mobility of the particles, especially for smaller particle size.[13]

2.1.3. Viscosity of solvent

Solvent viscosity is an important parameter in the EPD process. According to Henry equation, the viscosity of a medium is inversely proportional to the electrophoretic mobility of the particles. A low-viscosity media are required for successful EPD process and high particle mobility.[14]

2.1.4. Conductivity of suspension

The conductivity of the suspension should be in a specific range in order to be favourable for deposition and should be adjusted to maintain the mobility of the specific by tunning the excessive number of ions. Electrophoretic mobility and suspension conductivity are inversely proportional.[15] When the conductivity is very large, the particles move slowly (reduced electrophoretic mobility). On the other hand, when the conductivity is low, the suspension loses stability due to the deficit of a particle surface charge.[16,17]

2.1.5. Zeta potential

One of the key parameters of the EPD process is the zeta potential or electrokinetic potential of charged particles in solution. Zeta potential is the difference in electrical potential that is established within the interphase between the most outer part of the electric double layer formed at the surface of the particle and a solid/liquid interface.[18] It is closely related to the surface properties of suspended particles and medium ionic composition. Direct measurement of the absolute charge on the particles in a liquid media related to an electric double layer established is not possible. Zeta potential can be calculated from experimental data using the Helmholtz–Smoluchowski equations. Zeta potential is of great practical importance for colloidal chemistry and the behaviour of solid particles

suspended/dispersed in liquids. For example, higher zeta potential indicates that particles are stable in dispersion, while lower values of zeta potential indicate lower stability of charged particles in a suspension. When zeta potential reaches a value of zero (isoelectric point) particles will agglomerate and coagulation will occur. It is possible to measure the adsorption of other molecules and modification of the particle surface by measuring the change of their zeta potential in different media. Additionally, in a few studies, the toxicological potential of nanoparticles was correlated with their zeta potential values. It is clear that zeta potential is of great practical importance for electrophoresis and colloidal chemistry.[19]

2.1.6. pH of the suspension

One of the parameters on which zeta potential depends is pH due to high conductivities of hydrogen and hydroxide ions. If an alkali is added to a suspension containing particles with moderate negative zeta potential, the particles tend to acquire a more negative charge. If acid is added to this suspension, neutralization will occur, and consequently coagulation, or even precipitation, takes place. Similarly, adding more acid will generate a positive charge. Therefore, the zeta potential is positive at low pH values and negative at high pH values.[20] At higher concentrations, the acid or base will generate more charged particles in the double layer, which will increase the absolute zeta potential.

2.2. Parameters related to the process

2.2.1. Deposition time

One of the most important parameters of the EPD process is the deposition time. At constant voltage, the deposition rate during the EPD process is constant at the beginning and then decreases. This phenomenon is explained by the formation of an insulating layer (coating) on the electrode, which reduces the strength of the electric field.[21] It is crucial to determine the optimal deposition time to obtain a homogeneous coating without cracks at the defined deposition rate.[22]

2.2.2. Applied voltage

Although the amount of coating increases with increasing voltage, this increase deteriorates the coating uniformity. The application of high-strength electric field accelerates the deposition of particles, which does not allow them to pack uniformly within the coating. Additionally, the application of high voltages can increase the currents related to side electrochemical reactions such as hydrogen evolution reaction (cathodic), and oxygen evolution reaction (anodic), which will lead to pronounced release of H_2 and O_2 microbubbles and local change in pH which will cause cracking of the coating and its mechanical instability.

To avoid these issues, it is suggested to use moderate voltages.[23] It was also determined that the increase in applied voltage increases the surface roughness.

At low voltages, large particles cannot reach the substrate, and a uniform coating consisting of small particles is formed. By increasing the applied voltage, the particles move faster, which results in the formation of a less uniform coating consisting of large and small particles. In anaphoretic processes at passivating substrates, there is another issue of the increased rate of anodization of substrate at high voltages that will lead to simultaneous roughing of substrate and deposition of the rough coatings.[24]

2.2.3. Conductivity of substrate

The conductivity of the substrate can affect the quality of the coating obtained by the EPD process. Low substrate conductivity results in non-uniform coating and slow deposition. Longer deposition times are required to coat poor-conductive substrates compared to conductive ones. This is explained by the decrease in the electric field similar to the presence of a separator introduced in modified EPD processes.[25]

2.2.4. Concentration of a solid phase in the suspension

In general, the mass/thickness of the coating increase with increasing concentration. On the other hand, with an increase in thickness the cracks appear frequently, and the morphology of the coating is not uniform at a constant applied voltage.[26] In the case of multi-component systems, the partial rate of deposition depends on the volume fraction of particles in the suspension. When the volume fractions of solids is high, the particles are deposited at similar velocities. However, for small-volume fractions, the partial particle deposition rate depends on the electrophoretic mobility of each particle.[9]

3. KINETICS OF EPD PROCESS

Various attempts have been made to describe the kinetics of the EPD process. Hamaker[27] gave the first model of EPD kinetics for electrophoretic cells with planar geometry (Eq. (2)).[28] According to Hamaker, the deposited mass (m) is proportional to the solid phase concentration of the suspension (C_s), particle electrophoretic mobility (μ), the electrode surface area (S), the strength of the applied electric field (E) and deposition time (t):

$$m = C_s \mu S E t \tag{2}$$

Avgustinik *et al.*[29] checked Hamaker's law of deposition on a cylindrical electrode with a coaxial counter electrode and came up with modified equation for m in which the electrophoretic mobility is represented in terms of the permittivity of the suspending medium ($\varepsilon = \varepsilon_r \varepsilon_0$), the zeta potential ($\zeta$), and the viscosity of the solvent (η):[30]

$$m = \frac{lV|\zeta|\varepsilon C_s t}{3|\ln(a/b)|\eta} \tag{3}$$

where V is the voltage, l and a are the length and radius of the cylindrical electrode, respectively and b is the radius of the counter electrode ($b > a$).

Hamaker's equation is applicable only for short deposition times because the linear variation of deposited mass with deposition time in Eq. (2) implies that all other parameters are constant during deposition. In order to consider other experimental conditions, Sarkar and Nicholson[31] proposed that for infinitesimal time intervals, the modified Hamaker equation holds:

$$\frac{\partial m}{\partial t} = f C_s \mu S E \tag{4}$$

where $f \leq 1$ is the efficiency factor suggesting that not all particles brought to the electrode surface will precipitate, *i.e.*, if all the particles reaching the electrode surface are incorporated in the deposit: $f = 1$.[17] Based on this assumption, the authors modelled the variation of the deposited mass as a function of time for four different conditions, which are shown in Fig. 1.

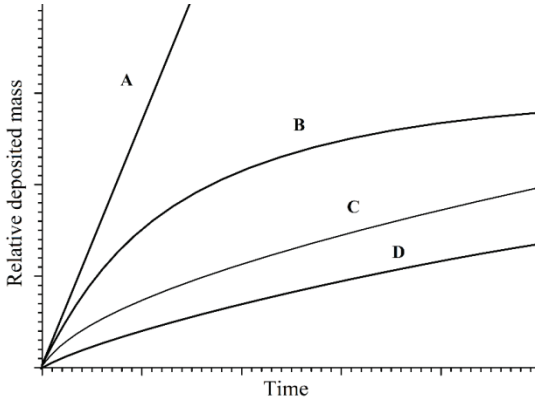

Fig. 1. Deposited mass as a fraction of C_s during EPD for four different deposition conditions: A) constant EPD current/constant concentration of suspension; B) constant EPD current, $dC_s/dt < 0$; C) constant EPD voltage/ /constant concentration and D) constant EPD voltage, $dC_s/dt < 0$.[31]

A comparison of curves A and C leads to the conclusion that the rate of deposition for curve C (constant voltage) decreases initially, whereas it remains constant in curve A (when deposited under constant current regime), and the coating yield in curve A case is significantly higher. This deviation of curve C from curve A is a consequence of the formation of the insulating layer of the coating which weakens the imposed electric field. This insulating layer causes significant voltage drop per unit depth of the suspension, with the current decreasing during deposition at constant voltage (curve C).

Biesheuvel and Verweij[30] presented the following equation for deposit growth, based on the Kynch theory of sedimentation[32] which describes the bulk effect of the particle motion in the transport phenomena near the deposition electrode and it is based on the expression of the mass balance of the suspension––deposit boundary evolution:

$$\frac{\partial \delta}{\partial t} = -v\frac{\phi_s}{\phi_d - \phi_s} \tag{5}$$

where δ is the coating thickness, v is the electrophoretic velocity of particles close to the electrode, ϕ_s is the volume fraction of the solid phase in the suspension, and ϕ_d is the volumetric parameter related to the deposit. For highly concentrated suspensions ($\phi_s > 0.2$), a correction factor (X):

$$X = \frac{\varphi_d}{\varphi_d - \varphi_s} \tag{6}$$

can be included in the kinetic expression, and original Hamaker equation, Eq. (2), transforms into:

$$\frac{\partial m}{\partial t} = f C_s \mu S E \frac{\phi_d}{\phi_d - \phi_s} \tag{7}$$

The expression for the strength of the electric field as a function of suspension conductivity (Λ) is:[33]

$$E = \frac{I}{\Lambda S} \tag{8}$$

where I is the particle migration current.

Finally:

$$\frac{\partial m}{\partial t} = f \mu C_s \frac{I}{\Lambda} \frac{\phi_d}{\phi_d - \phi_s} \tag{9}$$

To calculate the yield, Eq. (9) must be solved numerically. The accuracy of this equation was established using experimental data collected during the deposition.

Besides the direct current-EPD (DC-EPD) method where the deposition of charged particles occurs on the oppositely charged electrode in suspension under the influence of constant electric field there is the alternating current-EPD (AC--EPD) method in which the applied voltage is supplied from an AC field. In AC--EPD technique, the direction of electric field is reversed periodically which accounts for oscillation and migration of powder particles in the suspension between electrodes. It was shown that AC-EPD method leads to denser and less cracked coatings as compared to DC-EPD at similar thickness, having broader particle size distribution due to controlled particle migration according to the wave asymmetry and frequency. Fine tuning the asymmetry of AC wave as well as the frequency can further improve the coating characteristics.[34,35] Most models that explain the kinetics of the EPD process are based on the DLVO theory. This theory is named after the researchers Derjaguin, Landau, Verwey

and Overbeek.[36,37] According to this theory, the stability of suspended particles is determined by the interaction between attractive van der Waals forces and repulsive electrostatic forces between particles. At appropriate values of the ionic strength, the electrostatic stabilization of the colloid occurs. On the other hand, another important factor should be taken into account in the presence of hydrophilic polymers. In this case, the adsorption of macromolecules on the particles causes the repulsive forces between them and lead to steric stabilization.[38]

4. A NOVEL *IN SITU* METHOD OF ANODIZATION/ANAPHORETIC DEPOSITION OF CALCIUM PHOSPHATE COATINGS

Cataphoretic deposition of hydroxyapatite (HAp) coatings on titanium is a well-known and widely used method.[39] However, the disadvantage of this type of deposition is the poor adhesion of the coating to the substrate. Cataphoretic coatings are usually sintered to overcome this issue.[40] Sintering of the coating increases the strength of the metal–ceramic bond. This involves generation of an oxide interlayer by the oxidation of Ti substrate, which permeates into the deposited coating. It should be noted that HAp is sensitive to high temperatures because it decomposes into different calcium phosphate structures. Hence the curing by sintering is not rational procedure to improve the coating adhesion.

Another issue in the production of HAp coatings on Ti substrate is the low compatibility of physicochemical properties between these two materials. This causes poor bonding at the HAp/Ti substrate interface, which will lead to the depletion of the coating from the substrate, and consequently to an acceleration of the corrosion and biodegradation, as well as deterioration of the mechanical properties. Many different substrate surface modification techniques, such as anodization, chemical substrate treatment, spraying, *etc.*, have been investigated to overcome poor coating adhesion.[41] Anodization of the substrate surface is one of the most commonly used methods due to its simplicity. In many studies, this method has been used to obtain microporous films of titanium oxide on the substrate surfaces for orthopedic applications.[42] In order to improve the adhesion of the HAp coating on the Ti substrate, Parcharoen *et al.*[43] first treated the Ti surface with alkali and then anodized it before applying the coating on the Ti by an EPD process. However, in the literature, it is difficult to find any data related to the simultaneous processes of modification of the surface of Ti substrate and EPD application of the HAp coating.

Pantović Pavlović *et al.*[44–49] have presented a new method of applying calcium phosphate and hybrid coatings based on calcium phosphate ceramics on Ti substrates. The method is based on the electrophoretic deposition of calcium phosphate coatings. What is unique about this method is the synergy and simultaneous enactment of several processes. The first process is the anodization of the substrate surface, during which a passive oxide layer is formed on the surface

(TiO_2), which changes the surface structure and increases the surface roughness. Another process that takes place in parallel is the deposition of a calcium phosphate coating onto substrate. Another novelty of this coating synthesis approach is the application of anaphoretic deposition, which means that the suspension contained negatively charged particles that were deposited on the working anode, *i.e.*, substrate (Fig. 2). Joint anaphoresis/substrate anodization process was performed by applying different voltages, namely 30, 60 and 90 V during the anodization process while keeping the applied electric charge on the anode constant. The polished sample surface appears smooth and homogenized. As the anodization voltage increases, the surface roughness increases for 30 and 60 V, respectively. Although the roughness appears higher for 90 V than for 60 V, some flattening of the surface occurs. This flattening is confirmed by linear and surface roughness analyses.[44]

The pH value of the suspension was 10, which is another difference in comparison to cataphoretic deposition where, in order to stabilize the suspension, the pH value is adjusted to very acidic pH values.

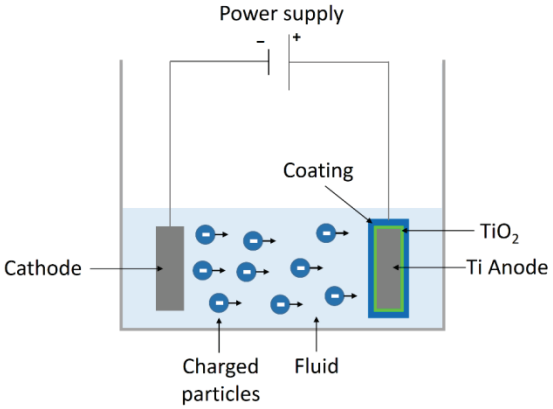

Fig. 2. Schematic representation of anaphoretic deposition.

For synthesized HAp/TiO_2 composite coating on a Ti substrate, using this new *in situ* method of anodization/anaphoretic deposition of calcium phosphate coatings to strengthen the biocompatible composite coating, there is no need for a subsequent treatments to cure adhesion.

Fig. 3 displays SEM microphotographs of catHAp and anHAp/TiO_2 coatings deposited via joint anaphoresis/substrate anodization process. As shown in Fig. 3a, the cataphoretically deposited HAp coating exhibits a large number of cracks. The granular structure of the catHAp coating can be observed in greater detail in Fig. 3b at higher magnification. These cracks are primarily caused by the mismatch in Young's modulus between the substrate and the coating. The titanium substrate is more elastic than the hydroxyapatite film, and as ceramic suspensions typically lose water content during drying, cracks in pure hydroxyapatite coatings

are inevitable. This water release occurs near the interface between the ceramic and the substrate, as well as within the bulk material, resulting in shrinkage of the ceramic coating surface and the formation of cracks even at low temperatures. It was found that catHAp coatings have very poor adhesion when deposited onto untreated Ti surfaces. Fig. 3c shows the SEM image of anHAp/TiO_2 composite coating on titanium deposited deposited *via* joint anaphoresis/substrate anodization process, while Fig. 3d displays the detailed morphology of the composite coating, with needle-like and granular HAp shapes at higher magnification. The deposition of anHAp/TiO_2 is observed without any visible cracks, unlike catHAp. This is attributed to *in-situ* deposition of the anHAp/TiO_2 coating.

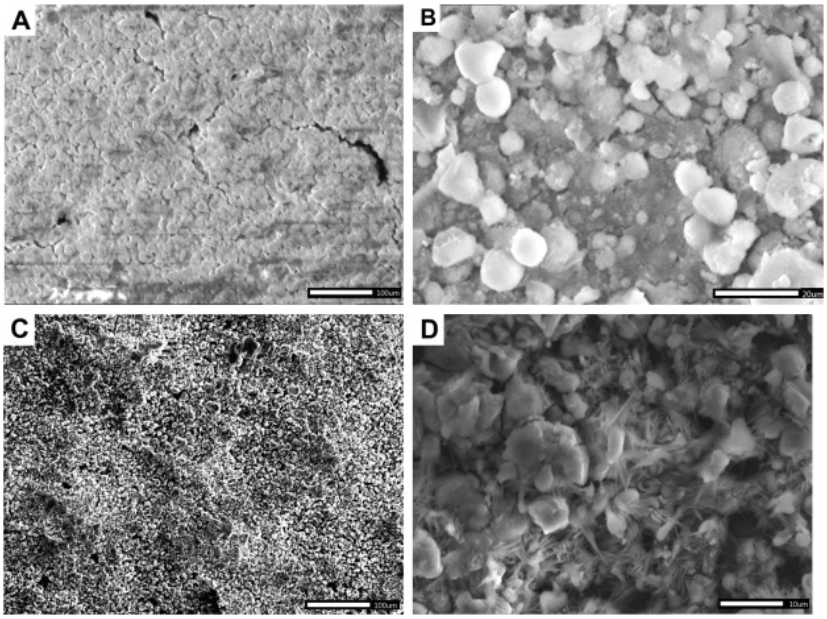

Fig. 3. SEM microphotographs of: a) catHAp coating, magnification ×200, b) catHAp coating, magnification ×1500, c) anHAp/TiO_2 coating, magnification ×200 and d) anHAp/TiO_2 coating, magnification ×2000.[45] Reprinted with permission from Elsevier.

Fig. 4 presents an FE-SEM microphotograph showing the morphology of the anaphoretically obtained HAp/TiO_2 composite coating (anHAp/TiO_2). On the surface of the coating, there are no visible cracks, unlike the cataphoretically obtained coating (catHAp). In Fig. 4, needle-like and granular forms of HAp can be observed, while catHap has a granular structure.[45]

It can be concluded that rational preparation of the suspension and the correct choice of electrolyte, which results in the creation of a stable negatively charged micelle, leads to the formation of a compact and durable coating on the substrate. The resulting coating shows good properties for potential use in bone

implants. The results showed that the new *in situ* process gives much better results than the cataphoretic deposition of HAp in terms of adhesion.[45] Fig. 5 shows a photograph of anHAp/TiO_2 composite coating after adhesion testing according to ASTM D3359-02 standard.

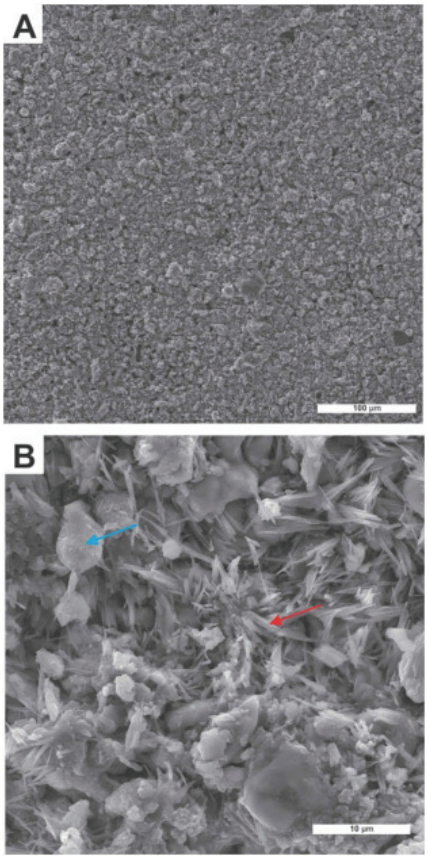

Fig. 4. FE-SEM microphotographs of composite anHAp/TiO_2 coating: a) magnification ×500 and b) magnification ×5000. Different HAp morphologies can be observed, blue arrow points granular and red one points needle-like HAp.[45] Reprinted with permission from Elsevier.

It was concluded that the adhesion of the anHAp/TiO_2 coating is level 4 compared to catHAp coatings which have adhesion level 1 or 2 even after the sintering process.[44] According to the ASTM D3359-02 standard, level 5 represents the best adhesion, while level 0 represents the worst adhesion.

Amorphous calcium orthophosphates (ACPs) are considered to be biomedically-relevant and bioactive calcium phosphates. ACPs possess adjustable chemical properties, but at the same time, they have glass-like physical properties with no long-range order in the atomic positions, whether orientational or translational, as described in reference[47]. Under certain conditions, ACPs can easily transform into thermodynamically stable hydroxyapatite. However, the stability

of ACPs and their transformation to crystalline HAp phases can be influenced by various additives and process parameters, as noted in reference.[47]

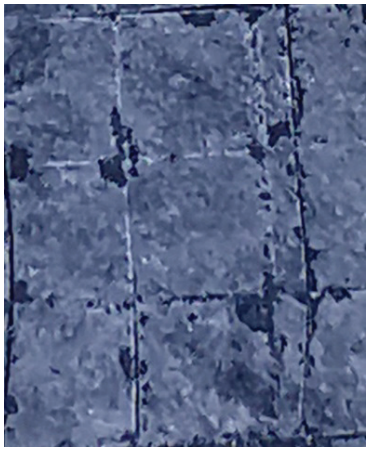

Fig. 5. Optical image of composite anHAp/TiO_2 coating after performing adhesion testing according to ASTM D 3359-02.[44]

The *in vitro* bioactivity of a substrate refers to its ability to form an apatite layer when in contact with biological or biological-like fluids. It was shown that the ACP/TiO_2 and ACP+ChOL/TiO_2 composites on Ti substrates can form a bone-like apatite layer on their surfaces when immersed in SBF solution. To assess the biocompatibility of these composite coatings, they were immersed in SBF solution and examined at different time intervals. The surface area physical appearance and particle size of the ACP/TiO_2 and ACP+ChOL/TiO_2 composite coatings on titanium substrates were characterized using SEM, along with the morphologies of the surfaces after immersion in SBF solution for various periods. Fig. 6a and b show the morphology of the ACP/TiO_2 and ACP+ChOL/ /TiO_2 composites surfaces before immersion in SBF solution, while Fig. 6c–f display the morphologies of the coatings immersed in SBF solution at different time periods.

The SEM images indicate that the composite coatings synthesized cover the substrate surface uniformly and consist of agglomerated nanosized particles with a size smaller than 100 nm. The ACP/TiO_2 and ACP+ChOL/TiO_2 coatings exhibit two different morphologies. The ACP/TiO_2 agglomerates appear larger, resulting in a coarser surface than the ACP+ChOL/TiO_2 coating. Additionally, small fractures are visible on the surface of the ACP+ChOL/TiO_2 composite coating, but it was found that the adhesion of these coatings is high, with a level of 5 according to ASTM D 3359-02: Standard Test Methods for Measuring Adhesion by Tape; cross-cut tape test (B), without any delamination or flaking. These findings suggest that pores are primarily formed during the one-step *in situ* anodization/anaphoretic electrodeposition process.[47]

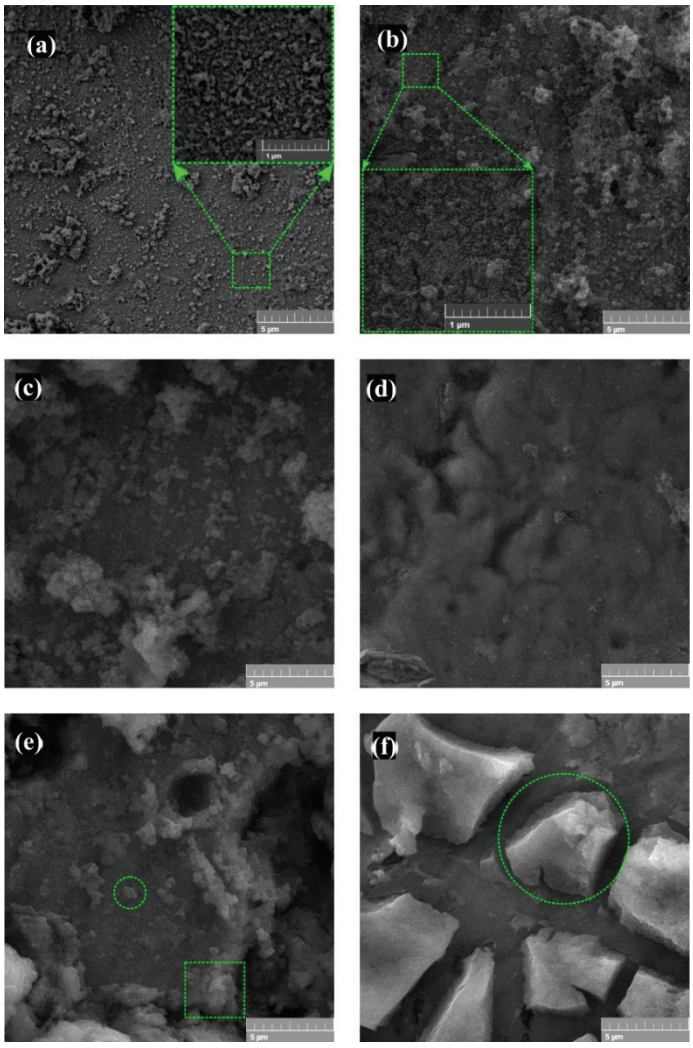

Fig. 6. FE-SEM micrographs presenting the morphology of: a) ACP/TiO_2 and b) ACP+ChOL/TiO_2 on Ti; ACP/TiO_2 coating on Ti immersed in SBF for: c) 72 and e) 240 h; ACP+ChOL/TiO_2 coating on Ti immersed in SBF for: d) 72 and f) 240 h.[47] Reprinted with permission from American Chemical Society.

The bioactivity of composite coatings of nano amorphous calcium phosphate/chitosan oligosaccharide lactate (ACP+ChOL)/titanium oxide (TiO_2) and ACP/TiO_2 after immersion in simulated body fluid (SBF) for 72 and 240 h is shown in Fig. 6c–f. XRD diffraction patterns of both coatings show broad amorphous peaks that can be assigned to ACP, while the ACP+ChOL/TiO_2 coatings also show peaks assigned to chitosan. After immersion in SBF, both coatings showed XRD peaks assigned to hydroxyapatite (HAp), which is an evidence of the coat-

ings' bioactivity. The ACP+ChOL/TiO_2 coating shows greater bioactivity than the ACP/TiO_2 coating, as it is completely covered with HAp after 72 h of immersion, whereas the ACP/TiO_2 coating takes 72 h to begin forming a new HAp layer, and it grows preferentially in a vertical rather than planar direction. The FE-SEM images of the coatings after 240 h of immersion in SBF show that both coatings are bioactive, with the newly formed HAp layer covering the entire surface of the coating. The ACP/TiO_2 coating has an uneven distribution of HAp particles, while the ACP+ChOL/TiO_2 coating has a smooth and even distribution, and also has the formation of rock-like structures of HAp, which indicates greater bioactivity and osteoconductivity.[47]

A cross-sectional SEM image and its corresponding EDS spectra in the case of ACP+ChOL/TiO_2 coating is presented in Fig 7a. Based on the information provided in Fig. 7a, it can be observed that the ACP+ChOL/TiO_2 coating has a compact structure with two distinct morphologies. The first morphology, labeled γ, belongs to the TiO_2 layer which forms instantaneously when the voltage difference is applied. The thickness of this layer is 170±15 μm, and the EDS spectra (Fig. 7-a2) show the presence of only Ti and O from TiO_2, along with some traces of Ca and P.

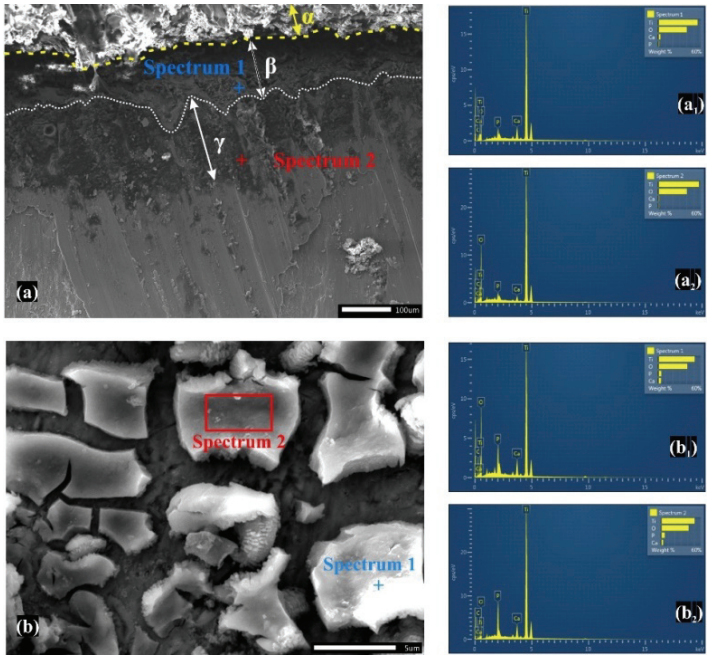

Fig. 7. Analysis of sample surfaces: a) SEM of cross-section of ACP+ChOL/TiO_2, a_1) EDS spectrum 1, a_2) EDS spectrum 2, b) SEM of ACP+ChOL/TiO_2 sample after immersion in SBF for 240 h, b_1) EDS spectrum 1 and b_2) EDS spectrum 2.[47] Reprinted with permission from American Chemical Society.

The second morphology, labeled β, belongs to the ACP+ChOL/TiO_2 coating and is 120±10 μm thick. Its deposition is a diffusion-limited process. The presence of ACP+ChOL in this layer can be inferred from the labeling, and it is confirmed by the EDS spectra. The top layer, labeled as α, belongs to the epoxy resin used to protect the coating while it was cross-cut for the analysis.

The EDS measurements in Fig. 7-b1 and b2 show the presence of both Ca and P, indicating the formation of hydroxyapatite ($Ca_{10}(PO_4)_6(OH)_2$) on the surface of the ACP+ChOL/TiO_2 and ACP/TiO_2 samples after immersion in SBF for 240 h. The Ca/P ratio of the ACP+ChOL/TiO_2 sample was 1.71 for spectrum 1 and 1.62 for spectrum 2, while the Ca/P ratio of the ACP/TiO2 sample was 1.63. Although the ideal Ca/P ratio for stoichiometric HAP is known to be 1.67, stable HAp phases have been found to exist over a range of Ca/P ratios between 1.3 and 1.8. The presence of C from ChOL can also be seen in both spectra in Fig. 7-b1 and b2. These quantitative EDS measurements are important for determining the elemental composition and Ca/P ratio of the synthesized films and confirming the formation of hydroxyapatite.

To summarize, the provided data describe the results of SEM and EDS analyses performed on ACP+ChOL/TiO_2 and ACP/TiO_2 coatings, both before and after immersion in SBF. The SEM images show a compact structure with two distinguishable morphologies – a TiO_2 layer formed instantaneously and an ACP+ChOL/TiO_2 coating formed *via* a diffusion-limited process.

Studies also showed that composite coatings of ACP/TiO_2 and ACP+ChOL/ /TiO_2 on titanium exhibit lower corrosion current density values in SBF solution compared to pure cp-Ti. The inclusion of ChOL in ACP solution improves the corrosion resistance by creating a stable, consistent coating on the titanium surface, resulting in a barrier layer that inhibits direct contact with the SBF solution. The ACP+ChOL/TiO_2 composite coating showed the lowest j_{corr} value (15.38×10^{-9} A cm^{-2}), which was approximately three times lower compared to the pure cp-Ti sample. The study suggests that the improved corrosion stability of the composite coatings can be attributed to the formation of both inhomogeneous and homogeneous oxides, as well as ceramic and composite layers.[47]

Above the mentioned, coating was further developed. Multifunctional hybrid coating on a titanium substrate that can promote controlled inflammation and immunomodulation at the implant-tissue interface was developed. The coating was composed of nano amorphous calcium phosphate and chitosan oligosaccharide lactate, and was decorated with selenium. *In situ* anodization/anaphoretic deposition was performed in order to create the coating, and then it was investigated for its immunomodulatory and anti-inflammatory effects *in vivo*. The study has found that the ACP/ChOL/Se multifunctional hybrid composite coating on a titanium substrate has an immunomodulatory and anti-inflammatory effect,

compared to pure grade 2 titanium implants that are commonly used in medicine and dentistry.[50]

5. CONCLUSION

A brief survey of the EPD process with a special attention on fundamental and applied aspects of the EPD process was described. The fundamental aspects were discussed with a focus on the basic principles of electrophoretic deposition and the kinetics of this process. The applied aspects of the EPD process were discussed with a focus on how practical process parameters influence the coating formation and its properties. The particular emphasis was given to the production of biocompatible HAp/Ti coatings produced by the EPD process on Ti substrate for biomedical applications. In the final section a novel process of anaphoretic deposition of HAp coatings on Ti was discussed. The advantage of novel HAp anaphoretic deposition coatings on Ti is the simultaneous oxidation of Ti substrates and the deposition of HAp coatings. As a result HAp coatings with better adhesion, biocompatibility and corrosion resistance are obtained when compared to cataphoretically produced HAp coating on Ti substrates. Novel anaphoretic deposition process of HAp coatings on Ti has excellent potential for further development through fundamental and applied aspects.

Acknowledgement. This work was supported by the Ministry of Education, Science and Technological Development of the Republic of Serbia (Grant No. 451-03-68/2022-14/ /200026).

ИЗВОД

АСПЕКТИ ПРИМЕНЕ ДВОЈНОГ ПРОЦЕСА АНАФОРЕЗЕ/АНОДИЗАЦИЈЕ СУПСТРАТА ЗА ФОРМИРАЊЕ БИОКОМПАТИБИЛНИХ КЕРАМИЧКИХ ПРЕВЛАКА

КАТАРИНА Ђ. БОЖИЋ[1,2], МИРОСЛАВ М. ПАВЛОВИЋ[1,2], ГАВРИЛО М. ШЕКУЛАРАЦ[1], СТЕФАН В. ПАНИЋ[1] и МАРИЈАНА Р. ПАНТОВИЋ ПАВЛОВИЋ[1,2]

[1]Институт за хемију, технологију и металургију, Институт од националног значаја за Републику Србију, Центар за електрохемију, Универзитет у Београду, Београд и [2]Центар изузетних вредности за хемију и инжењеринг животне средине, Институт за хемију, технологију и металургију, Београд

Електрофоретско таложење (EPD) може се јавити као катафоретско таложење – превлака се таложи на катоди, и анафоретско таложење – превлака се таложи на аноди. Примарна сврха EPD је добијање компактних и уједначених органских/неорганских превлака жељене дебљине и адхезије на металне површине применом електричног поља на честице прекурсора превлаке. Приказани су основни принципи EPD за наношење превлака који се односе на основна објашњења и разматрања практичних параметара процеса. Катафоретско таложење постало је популарно јер може нанети органске превлаке на сложене структуре на које је иначе веома тешко нанети превлаку. Утврђено је да ове превлаке побољшавају карактеристике подлоге, као што су биокомпатибилност, изглед и отпорност на процесе корозије. Кључни EPD параметри су састав, pH вредност и вискозност медијума за таложење, као и зета потенцијал честица, јачина електричног поља, итд. Посебан осврт је усмерен на процес анафоретског таложења, који је релативно нов, и његовим предностима. Расправља се и о катафоретском таложењу. Про-

цесом здруженог процеса анафорезе/анодизације супстрата, површина подлоге се истовремено анодизује и модификује уграђивањем честица превлаке у анодни слој. Добијају се превлаке мешовитог састава, боље адхезије и отпорности на корозију у односу на катафоретски нанесене превлаке.

(Примљено 18. јануара, ревидирано 10. фебруара, прихваћено 8. јула 2023)

REFERENCES

1. G. Choi, A. H. Choi, L. A. Evans, S. Akyol, B. Ben-Nissan, *J. Am. Ceram. Soc.* **103** (2020) 5442 (https://doi.org/10.1111/jace.17118)
2. J. Peña, I. Izquierdo-Barba, M. A. García, M. Vallet-Regí, *J. Eur. Ceram. Soc.* **26** (2006) 3631 (https://doi.org/10.1016/j.jeurceramsoc.2005.12.028)
3. B. D. Hahn, D. S. Park, J. J. Choi, J. Ryu, W. H. Yoon, J. H. Choi, H. E. Kim, S. G. Kim, *Surf. Coatings Technol.* **205** (2011) 3112 (https://doi.org/10.1016/j.surfcoat.2010.11.029)
4. I. Ullah, M. A. Siddiqui, H. Liu, S. K. Kolawole, J. Zhang, S. Zhang, L. Ren, K. Yang, *ACS Biomater. Sci. Eng.* **6** (2020) 1355 (https://doi.org/10.1021/acsbiomaterials.9b01396)
5. W. Yuan, J. Ji, J. Fu, J. Shen, *J. Biomed. Mater. Res., B* **85** (2008) 556 (https://doi.org/10.1002/jbm.b.30979)
6. N. Meyer, L. R. Rivera, T. Ellis, J. Qi, M. P. Ryan, A. R. Boccaccini, *Coatings* **8** (2018) 27 (https://doi.org/10.3390/coatings8010027)
7. L. Besra, M. Liu, *Prog. Mater. Sci.* **52** (2007) 1 (https://doi.org/10.1016/j.pmatsci.2006.07.001)
8. S. A. Batool, A. Wadood, S. W. Hussain, M. Yasir, M. A. Ur Rehman, *Surfaces* **4** (2021) 205 (https://doi.org/10.3390/surfaces4030018)
9. S. H. Lee, S. P. Woo, N. Kakati, D. J. Kim, Y. S. Yoon, *Energies* **11** (2018) 3122 (https://doi.org/10.3390/en11113122)
10. L. Kremser, D. Blaas, E. Kenndler, *Electrophoresis* **25** (2004) 2282 (https://doi.org/10.1002/elps.200305868)
11. A. Laska, M. Bartmański, *Inżynieria Mater.* **1** (2020) 20 (https://doi.org/10.15199/28.2020.1.3)
12. N. Sato, M. Kawachi, K. Noto, N. Yoshimoto, M. Yoshizawa, *Phys., C* **357**–**360** (2001) 1019 (https://doi.org/10.1016/S0921-4534(01)00510-X)
13. S. Cabanas-Polo, A. R. Boccaccini, *J. Eur. Ceram. Soc.* **36** (2016) 265 (https://doi.org/10.1016/j.jeurceramsoc.2015.05.030)
14. A. A. Sadeghi, T. Ebadzadeh, B. Raissi, S. Ghashghaie, *Ceram. Int.* **39** (2013) 7433 (https://doi.org/10.1016/j.ceramint.2013.02.087)
15. B. Ouedraogo, *J. Sci. Res. Reports* **2** (2013) 190 (https://doi.org/10.9734/jsrr/2013/2559)
16. B. Ferrari, R. Moreno, *Mater. Lett.* **28** (1996) 353 (https://doi.org/10.1016/0167-577X(96)00075-4)
17. B. Ferrari, R. Moreno, *J. Eur. Ceram. Soc.* **30** (2010) 1069 (https://doi.org/10.1016/j.jeurceramsoc.2009.08.022)
18. I. Aznam, J. C. W. Mah, A. Muchtar, M. R. Somalu, M. J. Ghazali, *J. Zhejiang Univ. Sci. A* **19** (2018) 811 (https://doi.org/10.1631/jzus.A1700604)
19. M. Předota, M. L. Machesky, D. J. Wesolowski, *Langmuir* **32** (2016) 10189 (https://doi.org/10.1021/acs.langmuir.6b02493)
20. S. Kamble, S. Agrawal, S. Cherumukkil, V. Sharma, R. V. Jasra, P. Munshi, *ChemistrySelect* **7** (2022) e202103084 (https://doi.org/10.1002/slct.202103084)

21. A. A. Abdeltawab, M. A. Shoeib, S. G. Mohamed, *Surf. Coatings Technol.* **206** (2011) 43 (https://doi.org/10.1016/j.surfcoat.2011.06.034)
22. I. Zhitomirsky, *J. Eur. Ceram. Soc.* **18** (1998) 849 (https://doi.org/10.1016/S0955-2219(97)00213-6)
23. R. N. Basu, C. A. Randall, M. J. Mayo, *J. Am. Ceram. Soc.* **84** (2001) 33 (https://doi.org/10.1111/j.1151-2916.2001.tb00604.x)
24. A. Rousta, D. Dorranian, *Trans. Inst. Met. Finish.* **99** (2021) 172 (https://doi.org/10.1080/00202967.2021.1914382)
25. P. Zhao, L. J. LeSergent, J. Farnese, J. Z. Wen, C. L. Ren, *Electrochem. Commun.* **108** (2019) 106558 (https://doi.org/10.1016/j.elecom.2019.106558)
26. A. M. A. Abudalazez, S. R. Kasim, A. B. Ariffin, Z. A. Ahmad, *Int. J. Eng. Res. Africa* **8** (2012) 47 (https://doi.org/10.4028/www.scientific.net/JERA.8.47)
27. H. C. Hamaker, *Trans. Faraday Soc.* **35** (1940) 279 (https://doi.org/10.1039/TF9403500279)
28. R. Moreno, B. Ferrari, in: *Electrophor. Depos. Nanomater.*, J.H. Dickerson, A.R. Boccaccini, Eds., Springer. New York, 2012, p. 73 (https://doi.org/10.1007/978-1-4419-9730-2_2)
29. A. I. Avgustinik, V. S. Vigdergauz, G. I. Zhuravlev, *J. Appl. Chem. USSR (Engl. Transl.)* **35** (1962) 2090 (https://jglobal.jst.go.jp/en/detail?JGLOBAL_ID=201602000824298251)
30. P. M. Biesheuvel, H. Verweij, *J. Am. Ceram. Soc.* **82** (1999) 1451 (https://doi.org/10.1111/j.1151-2916.1999.tb01939.x)
31. P. Sarkar, P. S. Nicholson, *J. Am. Ceram. Soc.* **79** (1996) 1987 (https://doi.org/10.1111/j.1151-2916.1996.tb08929.x)
32. G. J. Kynch, *Trans. Faraday Soc.* **48** (1952) 166 (https://doi.org/10.1039/tf9524800166)
33. G. Anné, K. Vanmeensel, J. Vleugels, O. Van Der Biest, *J. Am. Ceram. Soc.* **88** (2005) 2036 (https://doi.org/10.1111/j.1551-2916.2005.00387.x)
34. V. Ozhukil Kollath, Q. Chen, R. Closset, J. Luyten, K. Traina, S. Mullens, A. R. Boccaccini, R. Cloots, *J. Eur. Ceram. Soc.* **33** (2013) 2715 (https://doi.org/10.1016/j.jeurceramsoc.2013.04.030)
35. A. Braem, K. De Brucker, N. Delattin, M. S. Killian, M. B. J. Roeffaers, T. Yoshioka, S. Hayakawa, P. Schmuki, B. P. A. Cammue, S. Virtanen, K. Thevissen, B. Neirinck, *ACS Appl. Mater. Interfaces* **9** (2017) 8533 (https://doi.org/10.1021/acsami.6b16433)
36. E. J. W. Verwey, J. T. G. Overbeek, *Theory of the Stability of Lyophobic Colloids: The Interaction of Sol Particles Having an Electric Double Layer*, Elsevier, New York, 1948 (http://www.damtp.cam.ac.uk/user/gold/pdfs/teaching/BPFD/Chap2_10_VerweyOverbeek.pdf)
37. B. Derjaguin, L. Landau, *Prog. Surf. Sci.* **43** (1993) 30 (https://doi.org/10.1016/0079-6816(93)90013-L)
38. J. H. Adair, E. Suvaci, J. Sindel, in: *Encycl. Mater. Sci. Technol.*, K.H. Jürgen Buschow, R.W. Cahn, M.C. Flemings, B. Ilschner, E.J. Kramer, S. Mahajan, P. Veyssière, Eds., Elsevier, Amsterdam, 2001, p. 8996 (https://doi.org/10.1111/j.2042-7158.1951.tb13130.x)
39. S. Eraković, A. Janković, D. Veljović, E. Palcevskis, M. Mitrić, T. Stevanović, D. Janaćković, V. Miskovic-Stankovic, *J. Phys. Chem., B* **117** (2013) 1633 (https://doi.org/10.1021/jp305252a)
40. S. Erakovic, A. Jankovic, G. C. P. Tsui, C. Y. Tang, V. Miskovic-Stankovic, T. Stevanovic, *Int. J. Mol. Sci.* **15** (2014) 12294 (https://doi.org/10.3390/ijms150712294)

41. J. Li, P. Zhou, S. Attarilar, H. Shi, *Coatings* **11** (2021) 647 (https://doi.org/10.3390/coatings11060647)
42. C. Yao, T. J. Webster, *J. Nanosci. Nanotechnol.* **6** (2006) 2682 (https://doi.org/10.1166/jnn.2006.447)
43. Y. Parcharoen, P. Termsuksawad, S. Sirivisoot, *J. Nanomater.* **2016** (2016) 9143969 (https://doi.org/10.1155/2016/9143969)
44. M. R. Pantović Pavlović, M. M. Pavlović, S. Eraković, T. Barudžija, J. S. Stevanović, N. Ignjatović, V. V. Panić, *J. Serb. Chem. Soc.* **84** (2019) 1305 (https://doi.org/10.2298/JSC190730105P)
45. M. R. Pantović Pavlović, S. G. Eraković, M. M. Pavlović, J. S. Stevanović, V. V Panić, N. L. Ignjatović, *Surf. Coatings Technol.* **358** (2019) 688 (https://doi.org/10.1016/j.surfcoat.2018.12.003)
46. M. R. Pantović Pavlović, M. M. Pavlović, S. Eraković, J. S. Stevanović, V. V. Panić, N. Ignjatović, *Mater. Lett.* **261** (2020) 127121 (https://doi.org/10.1016/j.matlet.2019.127121)
47. M. R. Pantović Pavlović, B. P. Stanojević, M. M. Pavlović, M. D. Mihailović, J. S. Stevanović, V. V. Panić, N. L. Ignjatović, *ACS Biomater. Sci. Eng.* **7** (2021) 3088 (https://doi.org/10.1021/acsbiomaterials.1c00035)
48. M. R. Pantović Pavlović, M. M. Pavlović, J. N. Kovačina, B. P. Stanojević, J. S. Stevanović, V. V. Panić, N. L. Ignjatović, *J. Ser. Chem. Soc.* **86** (2021) 555 (https://doi.org/10.2298/JSC210211024P)
49. M. R. Pantović Pavlović, *PhD Thesis*, University of Belgrade, 2021 (in Serbian) (https://147.91.1.130/handle/123456789/4424)
50. M. R. Pantović Pavlović, N. L. Ignjatović, V. V Panić, I. I. Mirkov, J. B. Kulaš, A. L. Malešević, M. M. Pavlović, *J. Funct. Biomater.* **14** (2023) 227 (https://doi.org/10.3390/jfb14040227).